Graphane sheets and crystals under pressure

Xiao-Dong Wen[a,2], Louis Hand[b], Vanessa Labet[a], Tao Yang[a], Roald Hoffmann[a,1], N. W. Ashcroft[c], Artem R. Oganov[d,e], and Andriy O. Lyakhov[d]

[a]Department of Chemistry and Chemical Biology, Cornell University, Baker Laboratory, Ithaca, NY 14853-1301; [b]Department of Physics, Cornell University, Clark Hall, Ithaca, NY 14853-1301; [c]Laboratory of Atomic and Solid State Physics and Cornell Center for Materials Research, Cornell University, Clark Hall, Ithaca, NY 14853-2501; [d]Department of Geosciences and Department of Physics and Astronomy, State University of New York, Stony Brook, NY 11794-2100; and [e]Geology Department, Moscow State University, Moscow 119992, Russia

Contributed by Roald Hoffmann, February 25, 2011 (sent for review February 7, 2011)

Eight isomeric two-dimensional graphane sheets are found in a theoretical study. Four of these nets—two built on chair cyclohexanes, two on boat—are more stable thermodynamically than the isomeric benzene, or polyacetylene. Three-dimensional crystals are built up from the two-dimensional sheets, and their hypothetical behavior under pressure (up to 300 GPa) is explored. While the three-dimensional graphanes remain, as expected, insulating or semiconducting in this pressure range, there is a remarkable inversion in stability of the five crystals studied. Two stacking polytypes that are not the most stable at ambient pressure (one based on an unusual chair cyclohexane net, the other on a boat) are significantly stabilized with increasing pressure relative to stackings of simple chair sheets. The explanation may lie in the balance on intra and intersheet contacts in the extended arrays.

benzene isomers | high pressure | structural searching

A natural outgrowth of the synthesis of graphene (1–3) is an interest in chemically modified carbon sheets. Graphane is one of these—a fully saturated molecular (CH) sheet, four-coordinate at C.

This two-dimensional network was first suggested by Sluiter and Kawazoe (4), and by Sofo et al. (5), and synthesized in 2009 by Elias et al. (6) by exposure of a single-layer graphene to a hydrogen plasma [see also Ryu et al. (7); the extent of hydrogenation remains, to us, a problem in all syntheses to date]. It should be said right away that graphane, CH, is very much related to CF (carbon fluoride), a material with an older experimental and theoretical history (8–11). A number of structural proposals for graphane have antecedents in the fluorinated graphite literature. Certainly the graphane literature exploded after the Sofo et al. and Elias et al. papers; we mention here only several of the dozens of experimental and theoretical investigations of graphane that have followed (12–14).

Our interest in the field developed from another direction. We have been studying theoretically benzene (C_6H_6) under high pressure. The stoichiometry of the material is, of course, the same as that of graphane. In our calculations we first found that benzene phases under pressure underwent (at a certain pressure) phase transformation to saturated CH structures that were more stable. Among these more stable structures were graphanes. We report here the three-dimensional saturated CH graphane structures, some unique, that emerge from our theoretical work, and their computed behavior under pressure.

Results and Discussion

CH Structures from Evolutionary Structure Predictions. Once we found some saturated CH structures that were more stable than benzene, we began to look for more of them by evolutionary algorithm structure prediction, using the USPEX method/code (15–17) over the range of 0 to 300 GPa.

Five graphane stackings emerged as low in enthalpy at one or another pressure. These multilayer graphane structures are shown in Fig. 1. We call them:

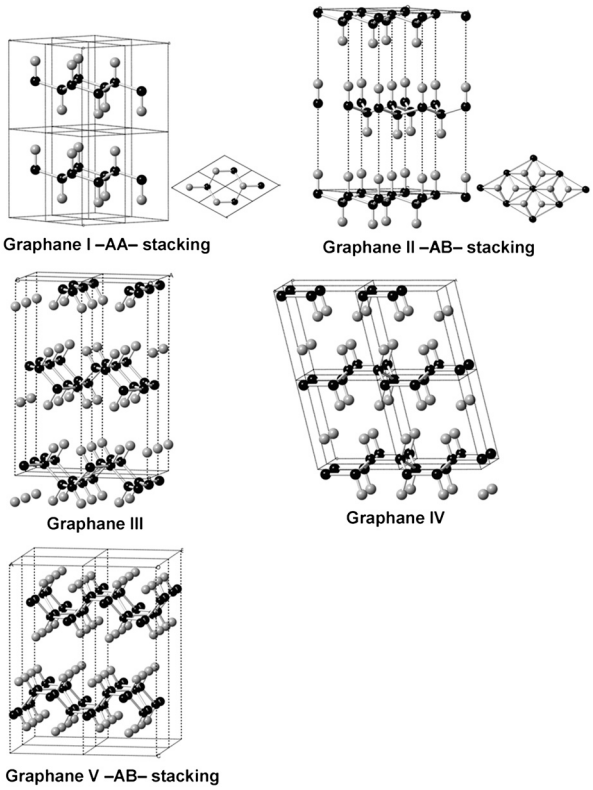

Fig. 1. Five multilayer graphanes structures at ambient pressure.

- graphane I (space group $P\text{-}3m1$, $Z = 2$, i.e., 2 CH in the unit cell, -AA- stacking),
- graphane II (space group $P6_3mc$, $Z = 4$, -AB- stacking),
- graphane III (space group $Cmca$, $Z = 8$)
- graphane IV (space group $P2_1/m$, $Z = 4$)
- graphane V (space group $Pnma$, $Z = 16$)

Note that just as for graphite, diamond, and SiC, there are many potential stacking polytypes built on any component sheet, e.g., -ABC-, -AABB- stacking and so on. These stackings were not explored by us; all of them are likely to be of similar enthalpy at ambient pressure to these five structures.

Author contributions: X.-D.W. and R.H. designed research; X.-D.W., V.L., and T.Y. performed research; A.R.O. and A.O.L. contributed new reagents/analytic tools; X.-D.W., L.H., V.L., R.H., and N.W.A. analyzed data; and X.-D.W., V.L., and R.H. wrote the paper.

The authors declare no conflict of interest.

[1]To whom correspondence should be addressed. E-mail: rh34@cornell.edu.

[2]Present address: Theoretical Division, Los Alamos National Laboratory, Los Alamos, NM 87545.

This article contains supporting information online at www.pnas.org/lookup/suppl/doi:10.1073/pnas.1103145108/-/DCSupplemental.

We proceeded to take these graphane crystals over a wide pressure range. But first we need to describe the structures in some detail, and this is best done by identifying precisely the component sheets.

Graphane Rafts. Fig. 2 shows four isomeric two-dimensional sheets of stoichiometry CH, labeled A ("chair1"), B ("chair2"), C ("boat1"), and D ("boat2"). These sheets may be derived by taking single-layer slices from the cubic and hexagonal diamond structures. Two of these structures, A and C, have a prehistory in the CF literature (9, 10). The chair2 layer, B, occurs also (not for carbon, and not as an isolated layer) in hundreds of inorganic compounds, such as $BaIn_2$ (18), TiNiSi (19), or EuAuSn (20). Layer B for graphane has also been suggested in the literature by several researchers (4, 21–24). Also Layer D, boat2, has been forwarded by Leenaerts et al. (22).

Potentially, there are many other isomeric graphane sheets. In a single six-carbon ring, if the position of a given hydrogen bonded to carbon is specified as U (up, above the six carbons) or D (down, below), then the following isomeric permutations are possible, written out linearly, but intended to be in a cycle (obviously there is also D/U permutational symmetry):

6 U: UUUUUU
5 U: UUUUUD
4 U: UUUUDD, UUUDUD, UUDUUD,
3 U: UDUDUD, UUDUDD, UUUDDD
2 U = 4U etc

To generate a viable net, not too strained, one can also couple an up/down pattern in one ring with another pattern in the adjacent ring: so structure C, boat1, couples UUDUUD in one ring with DDUDDU in two adjacent rings. Also, one of the less stable graphane sheets we found (structure F in the *SI Appendix* to this paper) combines 5U with 4U and 3U in adjacent rings. For an alternative enumeration, see the work of Sluiter and Kawazoe (4).

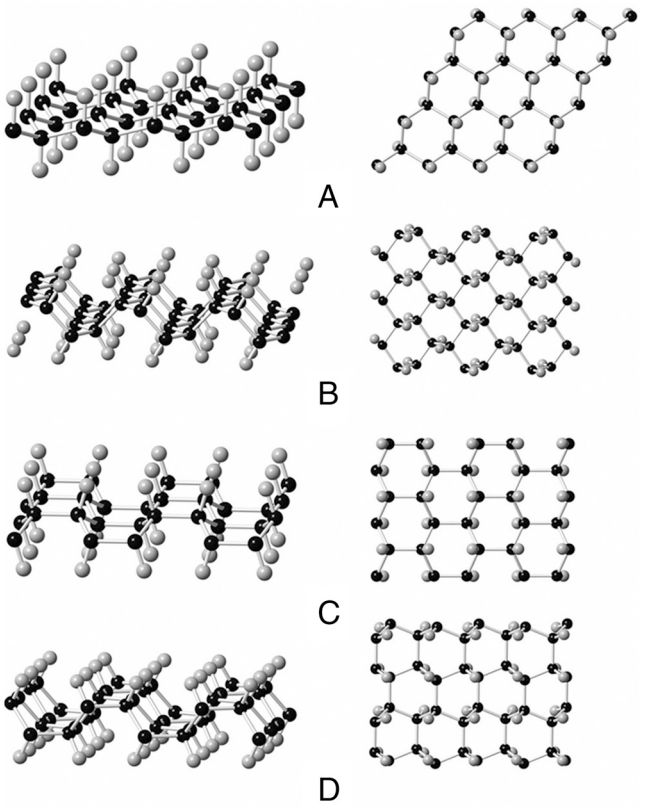

Fig. 2. Four isomeric single-sheet graphanes. Side views are at left, top views at right.

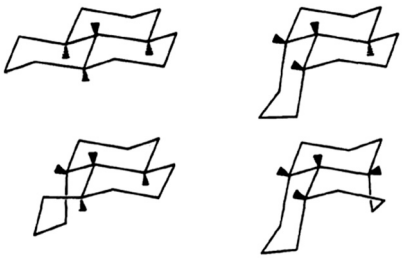

Scheme 1. Four isomeric tridecanes (8).

We have found realizations of each of the above possibilities, except for the unreasonably strained UUUUUU net where all hydrogens are on one side. A, B, C, and D of Fig. 2 are the most stable ones. Other CH rafts have been suggested in the literature (4, 23); we have found four others that are local minima. These last four nets are shown in the *SI Appendix* to this paper; they are very interesting, but all less stable than rafts A–D, and less stable per CH than benzene.

It is interesting to note here the smallest molecular models for the graphane sheets. These molecules are the isomers of $C_{13}H_{22}$, tricyclo[7.3.1.$0^{5,13}$]tridecanes or perhydrophenalenes; three of these have been synthesized (25, 26), and calculations of four isomers (Scheme 1) are also reported (27, 28).

We return to the four sheets most commonly invoked, A, B, C, and D. The factors entering the stability of such saturated hydrocarbons are well known in organic chemistry—they include (*i*) CCC angles, (*ii*) eclipsing and staggering interactions along the C-C bonds, and (*iii*) through-space steric interactions of hydrogens. Without any calculations, just based on the experience of organic chemistry, one would expect an energy ordering of A and B (chair cyclohexanes) more stable than C and D (boat). Moreover, we'd put A at lower energy than B, as B has some close H…H contacts between adjacent cyclohexanes.

Indeed the anticipated energy ordering is the one obtained for the $P = 1$ atm sheets, as Fig. 3 shows. In Fig. 3, we have also shown the benzene molecule and the *trans* and *cis*-polyacetylene structures. Zero point energies are not included in these calculations; they should be very similar in all the graphane structures

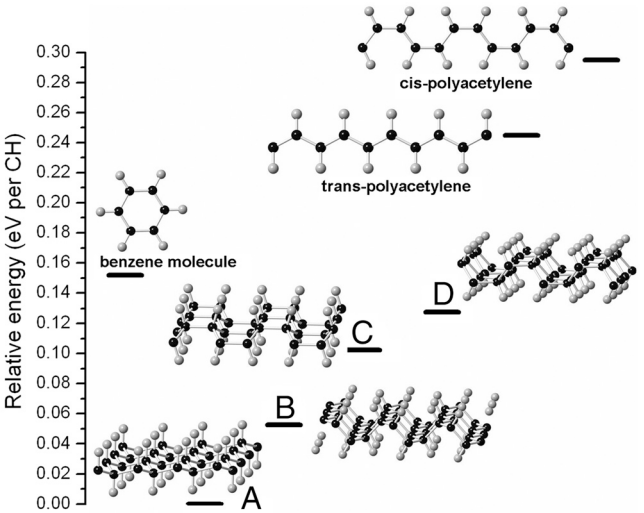

Fig. 3. The relative energy (in eV per CH; relative to single-sheet graphane A, 0 K) of some CH structures.

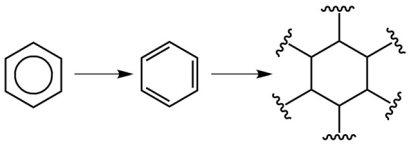

Scheme 2. Schematic formation of a four-coordinate C polymer from benzene. Note that hydrogens are omitted from this scheme.

considered here, as all of them have the same bonding patterns. Our energetic ordering agrees with calculations by others.

Note the graphanes A-D are all more stable than benzene, a result that was already obtained for two of these sheets by Sofo et al. (5). The argument for this order of stability, certainly surprising to organic chemists, is explored by us in detail elsewhere (29). Briefly, if we construct graphanes from benzene, as shown in the *Gedankenexperiment* of Scheme 2, the loss of aromaticity in the first step is overcome by the extra stability of CC σ over π bonds, afforded in the second stage of the construction.

The heat of formation of benzene is +0.173 eV/CH at 0 K (30). Thus the lowest enthalpy graphane layer, A, is slightly less stable than graphite and H_2.

Graphane Crystals. We now return to the stacking of these component two-dimensional graphane sheets into a three-dimensional crystal, the structures in Fig. 1. Fig. 4 shows the computed static lattice enthalpies of the graphanes as a function of pressure (up to 300 GPa). Because at $P = 1$ atm the three-dimensional structure adds only dispersion forces to the inherent stability of the two-dimensional sheets, we do not expect much difference, if any at all, between the energy ordering of the two-dimensional sheets and the three-dimensional crystal at $P = 1$ atm. Indeed we find graphane I, II (both built from chair1 sheet A) below III (from B), below IV (from C), and graphane V (built from D, -AA- stacking, the -AB-stacking is at higher energy).

The most stable phase we find in the range 0–10 GPa is the graphane I -AA- stacking or II -AB- stacking. Both stackings are dynamically stable (see *SI Appendix*), yet they are very close to each other in enthalpy, as expected at low pressures. At larger pressures a differential develops, favoring the -AB- stacking. There cannot be a large barrier to the sliding layer motion that changes one polytype into the other; not that different from sliding of the layers in graphite. By looking in detail at the sliding motion (leaving CC and CH distances fixed), we calculate essentially zero barrier to the -AA- to -AB- conversion at $P = 1$ atm, and 0.06 eV per CH at 10 GPa. The real barrier will be smaller.

Graphane III is the most stable phase in the range of 10–240 GPa. Above 240 GPa, graphane IV becomes the most stable

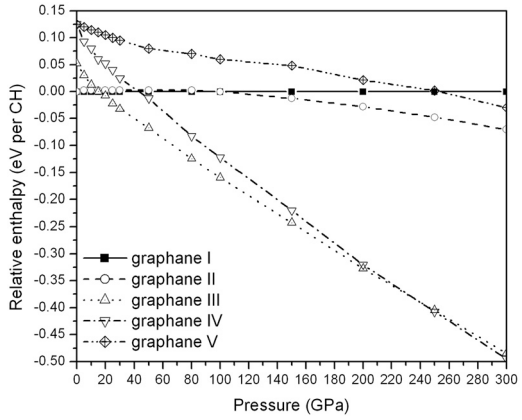

Fig. 4. Relative enthalpy (in eV per CH; relative to graphane I -AA-) of five three-dimensional graphane crystals as a function of pressure.

structure. The calculated phonon dispersions for graphane III and IV show no imaginary frequencies at 200 GPa and 300 GPa, indicating that both are dynamically stable (see *SI Appendix*). Graphane V does not compete with the other structures until 250 GPa, when it becomes more stable than I.

Transformations between graphanes {I or II} and III and IV are expected to have very large barriers, at any pressure. These sheets are not conformers, related to each other by mere C-C bond rotations. The various sheets are isomers—to convert one into another would involve breaking many CC bonds, and inverting hydrogens before reforming the bonds. So once a graphane crystal is made (for instance phase I or II), it will remain in that configuration as pressure is increased.

We have seen in the literature one attempt to estimate the barrier to transforming sheet A to C, for CF[11]. The barrier is estimated as 2.72 eV per CF by moving corresponding atoms. We have not yet studied this barrier for CH.

Some of the previous studies of graphane have calculated three-dimensional arrays. Ju et al (31) essentially calculated graphane I at $P = 1$ atm. Atryukhov and Chernozatonskii (24) explored stacking variants of layers A, B, and C at ambient pressure for CX (X = H, F). The energetic ordering of the layered structures in these studies matches the one we obtain, graphane I most stable.

In their important early study of CF, Charlier et al. (11) studied two stacking conformations of CF at ambient pressure—essentially the CF equivalent of our graphane I, and a boat stacking related to our graphane IV. Charlier et al. found the chair three-dimensional crystal of CF more stable than the boat one by 0.15 eV per CF, while we obtain 0.11 eV for CH.

Why the Change in Preferred Structure with Pressure? The layers in graphanes III and IV appear more "corrugated" than in graphanes I and II, and so would seem to mesh better on compression. But that supposition may be just wishful thinking, as layer D in graphane V is also corrugated. Of course, the calculated volume per layer follows the stability, with layers III and IV being more dense than the other graphanes.

As the pressure increases, the CC and CH distances (see *SI Appendix*) decrease in all structures. The range is CC = 1.54 Å at $P = 1$ atm to 1.36–1.38 Å at 300 GPa; CH = 1.10–1.11 Å at $P = 1$ atm to 1.01–1.02 Å at 300 GPa. The extent of bond compression in graphane sheets is similar to that calculated for diamond and methane over the same pressure range. The component cyclohexane rings all flatten, as indicated by the evolution of torsional angles (see *SI Appendix*).

Histograms of intra and interlayer H….H separations in the graphanes are informative. Fig. 5 shows these histograms for, by way of example, graphanes I and III at 1 atm and 300 GPa.

Note at $P = 1$ atm the shorter H….H intramolecular contacts for graphane III, disfavoring that crystal. However, at $P =$ 300 GPa, graphane I (and II) now has a very short intermolecular H….H contact, that works against that isomer. There are also signs that structure III adjusts its torsional angles "better" to the increased pressure, flattening more efficiently, to get hydrogens as much out of the interlayer space as possible (see *SI Appendix*).

Electronic Properties of Graphane Crystals. Just as methane and diamond remain insulators to very high pressures, we expect the three-dimensional graphane phases to do the same. Fig. 6 shows the band gap of four graphanes as a function of pressure. At ambient pressure, graphanes I–IV are calculated to be insulators with ~4 eV DFT (density functional theory) band gap. Hardly surprising for a saturated hydrocarbon.

The literature contains calculations of the electronic structure of single graphane sheets (5, 21–24), and of extended structures built from them (21, 23), all consistent with insulating or semiconducting behavior. Though normal DFT calculations, such as

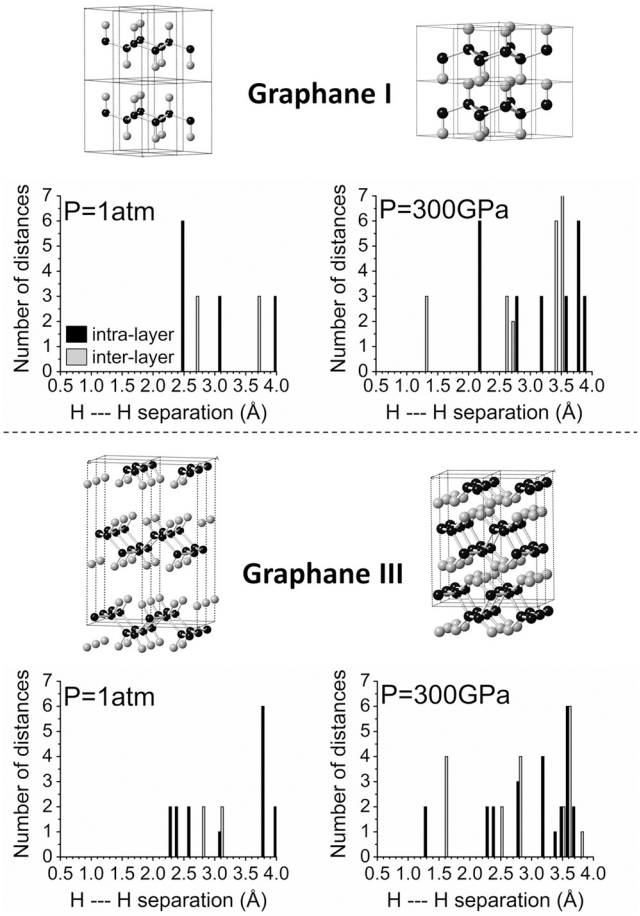

Fig. 5. Histogram of H-H distances in two graphanes (I and III) at 1 atm and 300 GPa.

we use, systematically underestimate band gaps (32). Thus the computed band gap of diamond at 1 atm is around 4.2 eV, which is lower than the experimental value at 5.5 eV.

It is interesting that the band gaps for the four graphanes increase at first with elevating pressure, and reach a maximum at ~20 GPa for I and II, and ~50 GPa for III and IV. Something similar also happens for diamond, where the band gap also initially rises with pressure and even the computed pressure derivative for the band gap is quantitatively similar, ~0.55 meV/GPa (33).

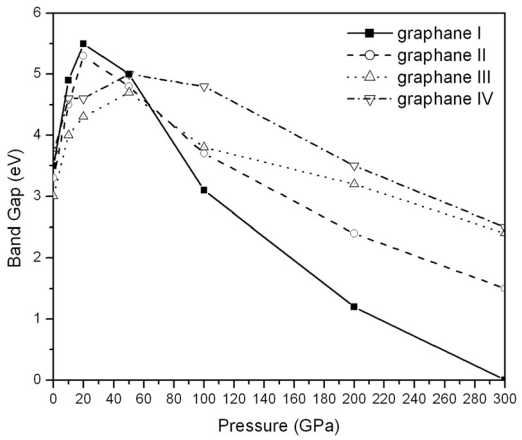

Fig. 6. Band gap of four graphanes as a function of pressure.

At higher pressures, the band gaps decrease. In our calculations, there is the usual correlation of band gap with stability (metals excepted)—less stable structures have smaller gaps between filled and unfilled bands/orbitals. Not much notice need be paid to graphane I going metallic at 300 GPa. Graphane I's true metallization pressure, like that of diamond, methane, and H_2, is likely to be higher.

The total density of states shows a characteristic free-electron-like shape (see *SI Appendix*) over a wide energy range at high pressure (>200 GPa).

Concluding Remarks

So, there is not one graphane sheet, but many. Coming to these remarkable saturated hydrocarbons from a starting point different from others studying them, we have found no less than eight graphane sheets that are dynamically stable. Four of them are more stable than benzene, the emblem of organic chemistry. In the three-dimensional crystals that can be built up from these sheets, we find an interesting change in stability with pressure. Whereas at $P = 1$ atm the chair-boat differential governs the energy differential among them, at higher pressures, e.g., 300 GPa, lattices built from two sheets that are not so stable at atmospheric pressure, chair2 and boat1, are enthalpically favored. We hazard an explanation.

Materials and Methods

The calculations are based on the plane-wave/pseudopotential approach using the computer program VASP (Vienna Ab-initio Simulation Package) (34), employing the PBE exchange-correlation functional (35, 36) and the projector-augmented wave (37, 38) method. The energy cutoff for the plane-wave basis was set to 600 eV. The Brillouin zone was sampled by Automatic-Mesh of 80 (automatically converted to Monkhorst-Pack meshes based on the structures' unit cell). We allowed all structural parameters (atomic positions, lattice constants) to relax. Phonon calculations were carried out using the linear-response method as implemented in the Quantum-ESPRESSO code (39). Pseudopotentials for H and C were generated by a Troullier-Martins norm-conserving scheme (40) and tested by comparing the optimized structural parameters and electronic structures with the results calculated from the VASP code. The evolutionary algorithm USPEX (15–17) with the fingerprint niching technique (41) was employed to find the lowest energy structures at 0, 5, 20, 50, 100, 200, and 300 GPa. In these calculations, we considered systems with up to 16 atoms in the unit cell, and used 30 structures in each generation, with 60% of the lowest-enthalpy structures allowed to produce the next generation through heredity (60%), lattice mutation (30%), and atomic permutation (10%); in addition, two lowest-enthalpy structures were allowed to survive into the next generation.

Supporting Information Available

In the *SI Appendix* we provide details of (*i*) structures of the single-sheet graphanes not shown in the body of the paper; (*ii*) phonon dispersion analysis of the graphanes; (*iii*) the computed total density of states for graphane III and IV at 200 GPa; (*iv*) the computed band structure and density of states of single-sheet graphanes at ambient pressure; (*v*) computed Wigner-Seitz radius r_s of diamond, graphane I, II, III, IV, V, and CH_4 and H_2; (*vi*) C-C and C-H distances in diamond, graphane I, II, III, IV, V, and CH_4 at 0–300 GPa; (*vii*) torsional angles in graphanes I, II, III, IV, and V at $P = 1$ atm and $P = 300$ GPa; (*viii*) enthalpy of stacked graphanes under high pressure; and (*ix*) a study of "releasing" pressure on some three-dimensional graphanes.

ACKNOWLEDGMENTS. We thank X-Q. Wang and D. K. Samarakoon for sending us information about two structures they suggested, to Andrey Rogachev for a careful reading and comments, and to Rodney Ruoff and Jorge Sofo for making us aware of the work of others. Our work at Cornell was supported by the National Science Foundation through Grant CHE-0613306 and CHE-0910623 and by EFree, an Energy Frontier Research Center funded by the Department of Energy, Office of Science, Office of Basic Energy Sciences under Award Number DESC0001057. A.R.O. thanks Intel Corp. for

financial support. This research was also supported by the National Science Foundation through TeraGrid resources provided by NCSA (National Center for Supercomputing Applications). Some calculations were performed in part at the Cornell NanoScale Facility, a member of the National Nanotechnology Infrastructure Network, which is supported by the National Science Foundation.

1. Novoselov KS, et al. (2004) Electric field effect in atomically thin carbon films. *Science* 306:666–669.
2. Dreyer DR, Ruoff RS, Bielawski CW (2010) From conception to realization: an historical account of graphene and some perspectives for its future. *Angewandte Chemie International Edition.* 49:9336–9344.
3. Boehm HP (2010) Graphene—how a laboratory curiosity suddenly became extremely interesting. *Angew Chem Int Ed* 49:9332–9335.
4. Sluiter MHF, Kawazoe Y (2003) Cluster expansion method for adsorption: application to hydrogen chemisorption on graphene. *Phys Rev B* 68:085410.
5. Sofo JO, Chaudhari A, Barber GD (2007) Graphane: a two-dimensional hydrocarbon. *Phys Rev B* 75:153401.
6. Elias DC, et al. (2009) Control of graphene's properties by reversible hydrogenation: Evidence for graphane. *Science* 323:610–613.
7. Ryu S, et al. (2008) Reversible basal plane hydrogenation of graphene. *Nano Lett* 8:4597–4602.
8. Watanabe N, Nakajima T, Touhara H (1988) *Graphite fluorides* (Elsevier, Amsterdam, New York).
9. Rüdorff W, Rüddorf G (1947) Zur Konstitution des Kohlenstoff-Monofluorides, Z. *Zeitschrift fur anorganische und allgemeine Chemie* 253:281–296.
10. Ebert LB, Brauman JI, Huggins RA (1974) Carbon monofluoride. Evidence for a structure containing an infinite array of cyclohexane boats. *J Am Chem Soc* 96:7841–7842.
11. Charlier JC, Gonze X, Michenaud JP (1993) First-principles study of graphite monofluoride $(CF)_n$. *Phys Rev B* 47:16162–16168.
12. Flores MZS, Autreto PAS, Legoas SB, Galvao DS (2009) Graphene to graphane: a theoretical study. *Nanotechnology* 20:465704.
13. Savini G, Ferrari AC, Giustino F (2010) First-principles prediction of doped graphane as a high-temperature electron-phonon superconductor. *Phys Rev Lett* 105:037002.
14. Cadelano E, Palla PL, Giordano S, Colombo L (2010) Elastic properties of hydrogenated graphite. *Phys Rev B* 82:235414.
15. Glass CW, Oganov AR, Hansen N (2006) USPEX—Evolutionary crystal structure prediction. *Computer Physics Communication* 175:713–720.
16. Oganov AR, Glass CW (2006) Crystal structure prediction using ab initio evolutionary techniques: principles and applications. *J Chem Phys* 124:244704.
17. Oganov AR, Glass CW, Ono S (2006) High-pressure phases of $CaCO_3$: crystal structure prediction and experiment. *Earth Planet Sci Lett* 241:95–103.
18. Nuspl G, Polborn K, Evers J, Landrum GA, Hoffmann R (1996) The four-connected net in the CeCu structure and its ternary derivatives. Its electronic and structural properties (1996). *Inorg Chem* 35:6922–6932 and references within.
19. Landrum GA, Evers JH, Boysen H, Hoffmann R (1998) The TiNiSi family of compounds: structure and bonding. *Inorg Chem* 37:5754–5763 and references within.
20. Bojin MD, Hoffmann R (2003) The REME phases: I. An overview of their structural variety. *Helv Chim Acta* 86:1653–1682 and references within.
21. Bhattacharya A, Bhattacharya S, Majumder C, Das GP (2011) The third conformer of graphane: a first principles DFT based study. *Phys Rev B* 83:033404.
22. Leenaerts O, Peelaers H, Hernández-Nieves AD, Partoens B, Peeters FM (2010) First-principles investigation of graphene fluoride and graphane. *Phys Rev B* 82:195436.
23. Samarakoon DK, Wang XQ (2009) Chair and twist-boat membranes in hydrogenated graphene. *ACS Nano* 3:4017–4020.
24. Artyukhov VI, Chernozatonskii LA (2010) Structure and layer interaction in carbon monofluoride and graphane: a comparative computational study. *J Phys Chem A* 114:5389–5396.
25. Pelter A, Maddocks PJ, Smith K (1978) Preparation of trans, trans, trans- and cis, cis, trans-Perhydrophenalen-9-ols by application of the three-migration cyanoborate process to isomeric perhydo-9b-boraphenalenes: differences between the cyanoborate and carbonylation reactions. *J Chem Soc Chem Comm* 18:805–806.
26. Brown HC, Dickason WC (1969) Synthesis of the cis, cis, cis-perhydro-9b-phenalenol, a very highly strained system, via the carbonylation reaction. High rate of solvolysis of the corresponding p-nitrobenzoate. *J Am Chem Soc* 91:1226–1227.
27. Gund P, Gund TM (1981) How many rings can share a quaternary atom? *J Am Chem Soc* 103:4458–4465.
28. Dillen JLM (1984) Conformational analysis of tricyclo[7.3.1.05,13]tridecane (perhydrophenalene) by molecular mechanics. *J Org Chem* 49:3800–3803.
29. Hoffmann R (2011) One shocked chemist. *Am Sci* 99:116–119.
30. Frenkel M, Marsh KN, Wilhoit RC, Kabo GJ, Roganov GN (1994) *Thermodynamics of Organic Compounds in the Gas State* (Thermodynamics Research Center, College Station, TX), See also http://cccbdb.nist.gov/hf0k.asp.
31. Ju WW, Wang H, Li TW, Fu ZY, Zhang QG (2010) First-principles study on the three-dimensional structure of graphane. *Key Eng Mat* 434–435:803–804.
32. Hafner J (2008) Ab-initio simulations of materials using VASP: density-functional theory and beyond. *J Comput Chem* 29:2044–2078.
33. Fahy S, Chang KJ, Louie SG, Cohen ML (1987) Pressure coefficients of band gaps of diamond. *Phys Rev B* 35:5856–5859.
34. Kresse G, Hafner J (1993) Ab initio molecular dynamics for liquid metals. *Phys Rev B* 47:558–561.
35. Perdew JP, Burke K, Ernzerhof M (1996) Generalized gradient approximation made simple. *Phys Rev Lett* 78:3865–3868.
36. Perdew JP, Burke K, Ernzerhof M (1997) Errata: generalized gradient approximation made simple. *Phys Rev Lett* 78:1396–1396.
37. Bloechl PE (1994) Projector augmented-wave method. *Phys Rev B* 50:17953–17979.
38. Kresse G, Joubert D (1999) From ultrasoft pseudopotentials to the projector augmented-wave method. *Phys Rev B* 59:1758–1775.
39. Giannozzi P, et al. (2009) QUANTUM ESPRESSO: a modular and open-source software project for quantum simulations of materials. *J Phys-Condens Mat* 21:395502.
40. Troullier N, Martins JL (1991) Efficient pseudopotentials for plane-wave calculations. *Phys Rev B* 43:1993–2006.
41. Lyakhov AO, Oganov AR, Valle M (2010) How to predict very large and complex crystal structures. *Computer Physics Communication* 181:1623–1632.